



Minerva Access is the Institutional Repository of The University of Melbourne

Author/s:

Xu, B;Anderson, BM;Mintern, JD;Edgington-Mitchell, LE

Title:

TLR9-dependent dendritic cell maturation promotes IL-6-mediated upregulation of cathepsin X

Date:

2024-10-01

Citation:

Xu, B., Anderson, B. M., Mintern, J. D. & Edgington-Mitchell, L. E. (2024). TLR9-dependent dendritic cell maturation promotes IL-6-mediated upregulation of cathepsin X. *Immunology and Cell Biology*, 102 (9), pp.787-800. <https://doi.org/10.1111/imcb.12806>.

Persistent Link:

<https://hdl.handle.net/11343/351396>

License:

[CC BY](#)

TLR9-dependent dendritic cell maturation promotes IL-6-mediated upregulation of cathepsin X

Bangyan Xu , Bethany M Anderson , Justine D Mintern  & Laura E Edgington-Mitchell  

Department of Biochemistry & Pharmacology, Bio21 Molecular Science and Biotechnology Institute, The University of Melbourne, Parkville, VIC, Australia

Keywords

cathepsin X, dendritic cells, IL-6, protease regulation, Toll-like receptors

Correspondence

Laura E Edgington-Mitchell, Department of Biochemistry & Pharmacology, Bio21 Molecular Science and Biotechnology Institute, The University of Melbourne, Parkville, VIC, Australia.

E-mail:

laura.edgingtonmitchell@unimelb.edu.au

Received 19 March 2024;
Revised 23 and 25 June 2024;
Accepted 26 June 2024

doi: 10.1111/imcb.12806

Immunology & Cell Biology 2024; **102**:
787–800

Abstract

Cysteine cathepsins are lysosomal proteases subject to dynamic regulation within antigen-presenting cells during the immune response and associated diseases. To investigate the regulation of cathepsin X, a carboxy-mono-exopeptidase, during maturation of dendritic cells (DCs), we exposed immortalized mouse DCs to various Toll-like receptor agonists. Using a cathepsin X-selective activity-based probe, sCy5-Nle-SY, we observed a significant increase in cathepsin X activation upon TLR-9 agonism with CpG, and to a lesser extent with Pam3 (TLR1/2), FSL-1 (TLR2/6) and LPS (TLR4). Despite clear maturation of DCs in response to Poly I:C (TLR3), cathepsin X activity was only slightly increased by this agonist, suggesting differential regulation of cathepsin X downstream of TLR activation. We demonstrated that cathepsin X was upregulated at the transcriptional level in response to CpG. This occurred at late time points and was not dampened by NF- κ B inhibition. Factors secreted from CpG-treated cells were able to provoke cathepsin X upregulation when applied to naïve cells. Among these factors was IL-6, which on its own was sufficient to induce transcriptional upregulation and activation of cathepsin X. IL-6 is highly secreted by DCs in response to CpG but much less so in response to poly I:C, and inhibition of the IL-6 receptor subunit glycoprotein 130 prevented CpG-mediated cathepsin X upregulation. Collectively, these results demonstrate that cathepsin X is differentially transcribed during DC maturation in response to diverse stimuli, and that secreted IL-6 is critical for its dynamic regulation.

INTRODUCTION

Cysteine cathepsin proteases are highly expressed by antigen-presenting cells, including macrophages and dendritic cells (DCs), where they govern innate and adaptive immunity in diverse ways. They regulate antigen uptake,¹ contribute to processing of antigenic peptides,^{2–7} and cleave invariant chain to promote MHC II maturation and antigen presentation.^{2,8} They also cleave and activate Toll-like receptors (TLRs),^{9–11} regulate cytokine secretion¹² and can promote inflammasome-mediated cell death when released into the cytosol.^{13,14} The expression of cathepsins in macrophages, especially in the context of a tumor microenvironment, is provoked by the T_H2-associated cytokines interleukin-4,

-6, -10 and -13, which act synergistically to promote STAT3- and 6-dependent transcription.^{15–17}

Cathepsin X (also cathepsin Z/P; gene name *Ctsz*) is a unique member of the cysteine cathepsin family, exhibiting strict carboxy-mono-exopeptidase activity.¹⁸ In DCs differentiated from peripheral blood of healthy volunteers, cathepsin X was shown to play important roles during maturation, adhesion, migration and cytokine secretion.¹⁹ In murine bone marrow-derived DCs, cathepsin X promotes inflammasome activation independent of its catalytic mechanism.^{20,21} In microglial cells, cathepsin X is secreted in response to the TLR agonists LPS and Poly I:C, where it may promote cytokine secretion and neuroinflammation.²²

We have previously shown that cathepsin X is active to a similar extent in cDC1 and cDC2 subtypes isolated from murine spleen.²³ Whether and how cathepsin X is regulated during DC maturation has not been previously investigated in detail. Using Mutu DCs, an immortalized murine DC line,²⁴ we therefore set out to profile cathepsin X activation in response to various TLR agonists and to examine the signaling mechanisms that regulate its expression. We demonstrate that cathepsin X is significantly upregulated in response to TLR9 agonism, and that this is governed by IL-6 secreted from mature DCs.

RESULTS

Cathepsin X is differentially regulated by TLR agonists during dendritic cell maturation

To study the regulation of cathepsin X activity during DC maturation, we used an activity-based probe, sCy5-Nle-SY (Supplementary figure 1a, b),²⁵ in Mutu DCs. As we reported previously in RAW264.7 macrophages, sCy5-Nle-SY covalently labels two proteases in Mutu DCs, as shown by in-gel fluorescence (Figure 1a). The identity of these species was verified to be cathepsin X (35 kDa) and cathepsin S (25 kDa) by immunoprecipitation of probe-labeled lysates with specific antibodies (Supplementary figure 1c). We demonstrated previously that the 35 kDa band is completely absent in cathepsin X-deficient Mutu DCs or cells only expressing catalytically dead cathepsin X, further validating its identity.²⁶ Moreover, pretreatment of the cells with MDV-590,²⁷ a cathepsin S-specific inhibitor, led to the complete loss of cathepsin S labeling (Supplementary figure 1d).

To investigate the impact of DC maturation on cathepsin activation, we stimulated Mutu DCs with six different TLR agonists, including Pam3 (TLR1/2), FSL-1 (TLR2/6), Poly I:C (TLR3), LPS (TLR4), R848 (TLR7/8) and CpG (TLR9). Cell surface expression of CD86 was measured by flow cytometry as an indicator of maturation (Supplementary figure 2a, b). The cells strongly responded to Pam3, FSL-1, Poly I:C and CpG. As observed previously,²⁴ Mutu DCs partially responded to LPS treatment, but not R848.

Compared with naïve DCs, CpG-treated cells exhibited significantly increased cathepsin X activity (11.2-fold, $P = 0.039$), while Pam3 and FSL-1 treatment increased cathepsin X activity to a lesser extent (4.7-fold, $P = 0.0009$ and 7.0-fold, $P = 0.026$, respectively). Although Poly I:C treatment induced DC maturation to a similar extent to CpG, Pam3 and FS-1, it had comparatively little impact on cathepsin X activity

(2.6-fold, $P = 0.0028$). In agreement with LPS only partially inducing DC maturation, this agonist slightly increased cathepsin X activity (2.3-fold, $P = 0.007$) (Figure 1a, b). Labeling of cathepsin S was only slightly increased by CpG (1.8-fold, $P = 0.0012$), but not by the other agonists (Figure 1c).

We next measured the total cathepsin X levels by immunoblotting with a cathepsin X-specific antibody, which showed a similar pattern to active cathepsin X (Figure 1a, d). These results suggest that cathepsin X is differentially regulated at the expression level upon TLR-induced DC maturation. Accordingly, mRNA expression of cathepsin X was significantly increased after CpG-treatment, as measured by RT-PCR (4.2-fold, $P = 0.0007$; Figure 1e). CpG treatment of primary CD11c⁺ DCs isolated from mouse spleen also provoked an increase (2.2-fold, $P = 0.001$) in total cathepsin X protein, mirroring the effect in Mutu DCs (Supplementary figure 3a–c).

CpG treatment upregulates both intracellular and secreted cathepsin X

By immunofluorescence, we examined the localization of cathepsin X in naïve and CpG-activated DCs. In agreement with the immunoblot, total cathepsin X levels were increased after maturation. In both naïve and CpG-treated cells, cathepsin X exhibited a punctate cytoplasmic distribution consistent with endolysosomal localization (Figure 2a). Previous studies have suggested a redistribution of cathepsin X to the membrane during maturation of pDCs.¹⁹ We did not observe this translocation in Mutu DCs; however, we did observe increased cathepsin X secretion upon CpG treatment (3.2-fold, $P = 0.0011$). In both naïve and mature DCs, cathepsin X was secreted primarily in the zymogen form, and thus minimal labeling by sCy5-Nle-SY was observed (Figure 2b).

We next demonstrated that the effect of CpG on active and total cathepsin X in Mutu DCs is concentration-dependent, with significant upregulation occurring as low as 0.04 μM and plateauing by 0.2 μM (Supplementary figure 4a). We also investigated the timing of cathepsin X regulation by CpG. Cathepsin X was not significantly increased after 8 h, but reached maximal levels at 24 and 32 h, and declined by 48 h (Figure 2c).

Lysosomal cysteine proteases and cystatin C are differentially regulated in response to TLR9 activation

We next aimed to examine whether upregulation in response to CpG treatment was specific to cathepsin X or a general feature of cysteine proteases. After live-cell

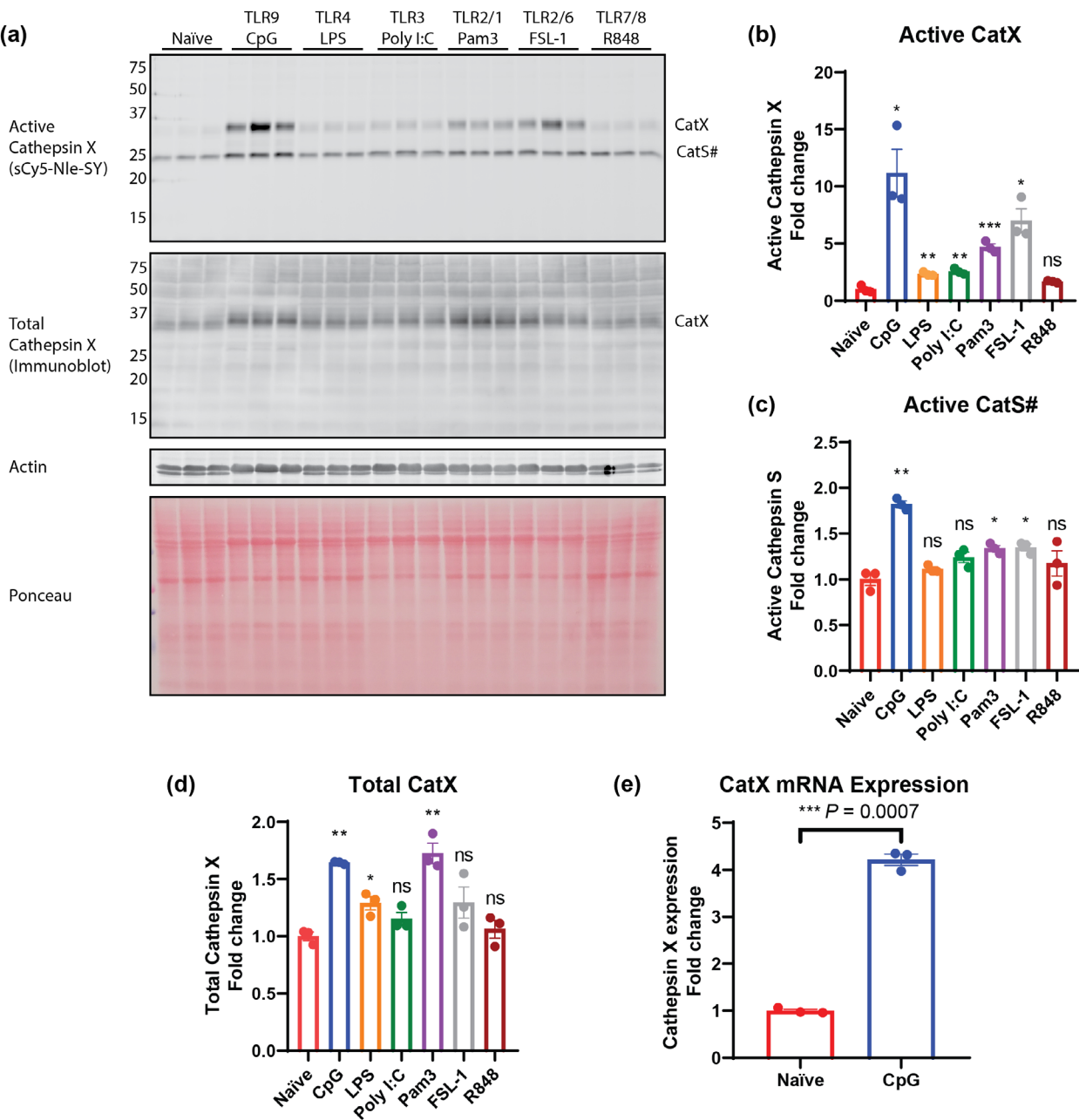


Figure 1. Cathepsin activation during dendritic cell maturation. **(a)** Mutu DCs were pre-treated with TLR agonists for 24 h, followed by live labeling with sCy5-Nle-SY and analysis by in-gel fluorescence. Total cathepsin X protein was examined by immunoblot. Actin blot and Ponceau stain were used to assess protein loading. Densitometry of active cathepsin X bands **(b)** and cathepsin S bands **(c)** displayed as the average intensity normalized to the average intensity of the naïve samples (fold change). Statistical analysis was performed using unpaired Student's *t*-tests. Three technical replicates of stimulated cells are shown, representative of > 3 separate experiments. **(d)** Densitometry of total cathepsin X bands displayed as the average intensity normalized to the average intensity of the naïve samples (fold change). Statistical analysis was performed using unpaired Student's *t*-tests. Three technical replicates of stimulated cells are shown, representative of > 3 separate experiments. **(e)** Quantitative PCR analysis of cathepsin X mRNA normalized to mouse GAPDH in naïve and CpG-treated Mutu DCs, reported as fold-change compared with naïve. Statistics were performed using the unpaired Student's *t*-test. Three technical replicates of stimulated cells are shown. Error bars represent SEM. ns $P > 0.05$, * $P \leq 0.05$, ** $P \leq 0.01$, *** $P \leq 0.001$. #This band may be a mixture of cathepsin S and another protease.

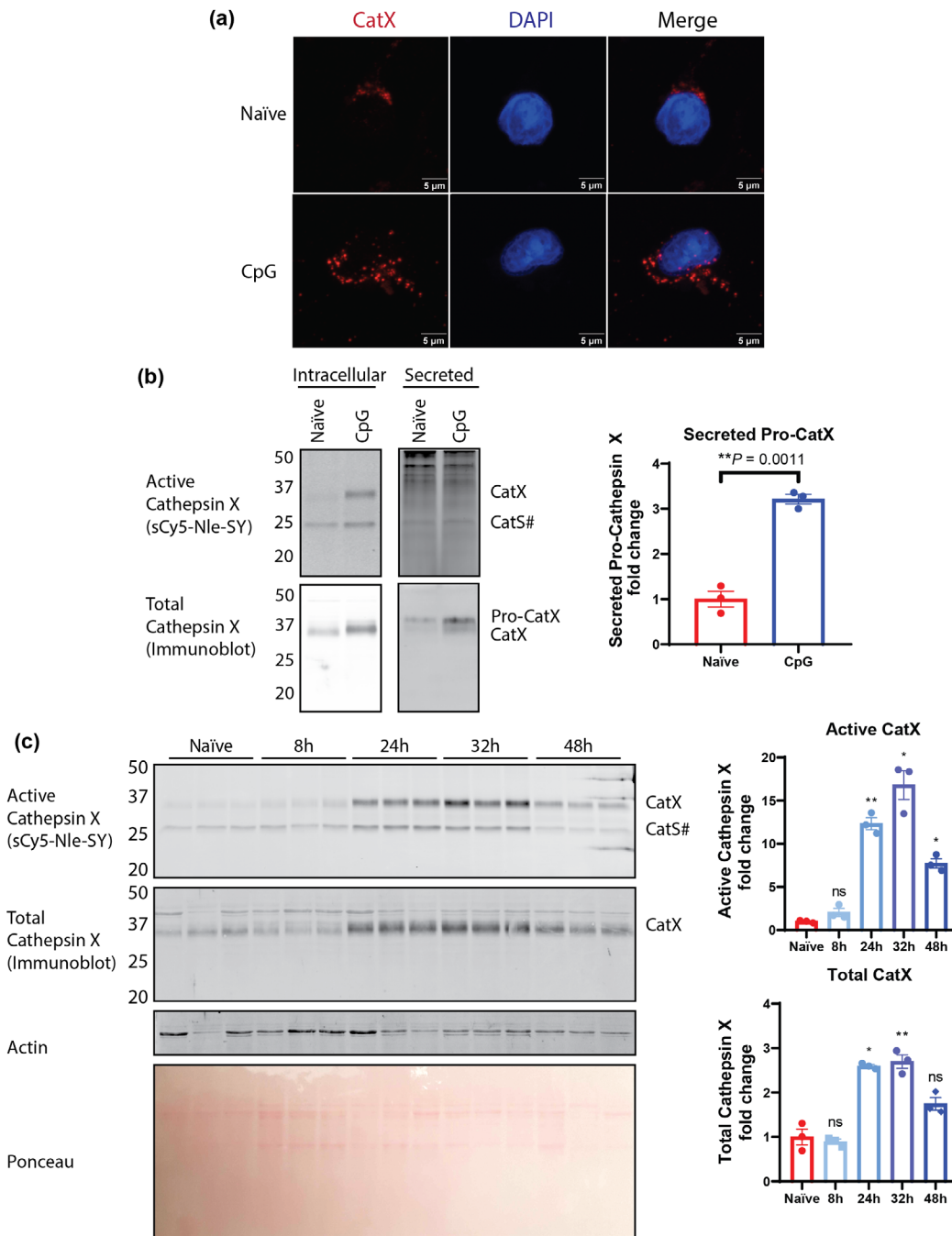


Figure 2. Alterations in cathepsin X levels during DC maturation. **(a)** Intracellular cathepsin X in naïve and CpG-treated Mutu DCs as shown by immunofluorescence. Scale bar = 5 μm. **(b)** Comparison of intracellular and secreted cathepsin X in naïve and CpG-treated DCs as shown by ingel fluorescence of sCy5-Nle-SY (active) and immunoblot (total). Densitometry of secreted pro-cathepsin X bands displayed as the average intensity for all naïve and treated cells relative to naïve cells (fold-change). Statistical analysis was performed using unpaired Student's *t*-tests. Three technical replicates of stimulated cells are shown, representative of > 3 separate experiments. **(c)** Time course of CpG-dependent cathepsin X upregulation, as shown by sCy5-Nle-SY labeling and immunoblotting. Actin and Ponceau stain were used to assess protein loading. Densitometry of active and total cathepsin X bands displayed as the average intensity for all naïve and treated cells, normalized to naïve (fold change). Statistical analysis was performed using Brown–Forsythe and Welch ANOVA tests. Three technical replicates of stimulated cells are shown, representative of two separate experiments. Error bars represent SEM. ns *P* > 0.05, **P* ≤ 0.05, ***P* ≤ 0.01. #This band may be a mixture of cathepsin S and another protease.

labeling with a pan-cysteine cathepsin ABP BMV109,^{28,29} which targets cathepsin B, L, S and X, we again observed increased levels of cathepsin X upon CpG treatment. Labeling of cathepsin B was much lower than cathepsin X and S in DCs, and cathepsin L was not consistently labeled by BMV109 (Figure 3a). By immunoblot, mature DCs showed increased pro- (~37 kDa) and single-chain cathepsin B (~30 kDa) upon CpG treatment (1.8-fold, $P = 0.0009$ and 2.2-fold, $P = 0.0014$, respectively). Pro- (~35 kDa) and single-chain cathepsin L (~27 kDa) also increased after CpG treatment (2.9-fold, $P = 0.0026$ and 5.4-fold, $P = 0.0011$, respectively). However, the heavy chain form of both cathepsin B and L remained unchanged (Figure 3a). Interestingly, cathepsin S activity detected by BMV109 was significantly decreased (0.48-fold, $P = 0.0001$) upon maturation, and this correlated with a decrease in total cathepsin S levels (0.41-fold, $P = 0.0004$) (Figure 3a). This is in direct contrast to the 25 kDa band labeled by sCy5-Nle-SY, which was slightly increased upon CpG treatment (Figure 1a). This suggests that there may be another protease labeled by sCy5-Nle-SY that both co-migrates with cathepsin S and binds to the cathepsin S-specific inhibitor. We have not yet successfully purified this species, which has precluded definitive proteomic identification. Alternatively, it is also possible that the two probes concentrate in different subcellular compartments, but this needs further investigation.

FY01,³⁰ a cathepsin C-selective probe, labeled multiple species in DCs, but we did not observe significant changes between naïve and CpG-treated cells. Total cathepsin C levels were also unchanged (Figure 3b). Using LE28, we measured the activity of another lysosomal cysteine protease legumain (asparaginyl endopeptidase).³¹ While legumain activity and total mature legumain remained unchanged, we observed increased pro-legumain (3.32-fold, $P = 0.0002$, Figure 3c). Finally, we examined the levels of cystatin C, an endogenous inhibitor of both cathepsins and legumain. In agreement with previous reports,³² cystatin C expression was strongly downregulated upon DC maturation (0.17-fold, $P = 0.016$, Figure 3d). Collectively, these data suggest that lysosomal cysteine proteases are differentially regulated by TLR9 agonism, with cathepsin X being the only protease exhibiting strong upregulation in both total and active levels.

Cathepsin X upregulation by CpG is not a direct result of NF- κ B activation or IFN activation

Having demonstrated that CpG treatment leads to robust upregulation of cathepsin X transcription in DCs, we

next sought to determine the mechanisms that govern its expression.

Activation of TLR9 leads to the translocation of NF- κ B into the nucleus, where it acts as a transcription factor to promote the expression of inflammatory genes.³³ As the cathepsin X gene promoter contains a putative NF- κ B binding site,³⁴ we queried whether cathepsin X transcription in DCs was NF- κ B-dependent. We used increasing concentrations of 6-amino-4-(4-phenoxyphenylethylamino) quinazoline to inhibit NF- κ B activation.³⁵ This inhibitor reduced the secretion of IL-6 (0.71-fold, $P = 0.0123$), IL-10 (0.38-fold, $P < 0.0001$) and TNF α (0.41-fold, $P < 0.0001$), indicating effective dampening of NF- κ B activity (Supplementary figure 5). It had no effect, however, on the upregulation of cathepsin X in response to CpG treatment (Figure 4a), suggesting that NF- κ B is not likely to be responsible for directly promoting cathepsin X transcription. This is in agreement with the observation that cathepsin X expression is induced at late time points (24 h; Figure 2c), whereas an NF- κ B-mediated transcriptional response would occur much earlier.^{36–38}

TLR9 signaling also leads to the activation of interferon regulatory factors (IRFs) and the expression of type I interferons, including IFN- α and IFN- β .³⁹ To investigate whether type I interferons could induce upregulation of cathepsin X, we stimulated DCs with IFN- α or IFN- β . We did not, however, observe significant changes between naïve cells and those treated with IFN- α or IFN- β (Figure 4b). Interestingly, we found that the type II interferon IFN- γ prevented the upregulation of cathepsin X by CpG (Figure 4c), despite the cells being more mature with the co-treatment than CpG alone.²⁴

Cathepsin X upregulation by CpG is IL-6-dependent

We next hypothesized that the factors secreted by DCs during CpG-mediated maturation function to promote cathepsin X expression. To test this hypothesis, we pulsed DCs with CpG for 3 h and then changed the media to wash out CpG. After 24 h, we collected the conditioned media containing secreted factors and applied it to naïve DCs for 24 h (Figure 5a). Active and total cathepsin X levels were significantly elevated in the cells treated with conditioned media compared with naïve cells (3.2-fold, $P = 0.0009$ and 1.5-fold, $P = 0.0457$, respectively; Figure 5b). This suggests that factors secreted from DCs downstream of CpG activation may be responsible for inducing cathepsin X expression.

Using a cytometric bead array, we quantified the major cytokines secreted by DCs during maturation. Upon CpG treatment for 24 h, the conditioned media contained high levels of TNF- α and IL-6 and a detectable level of IL-10

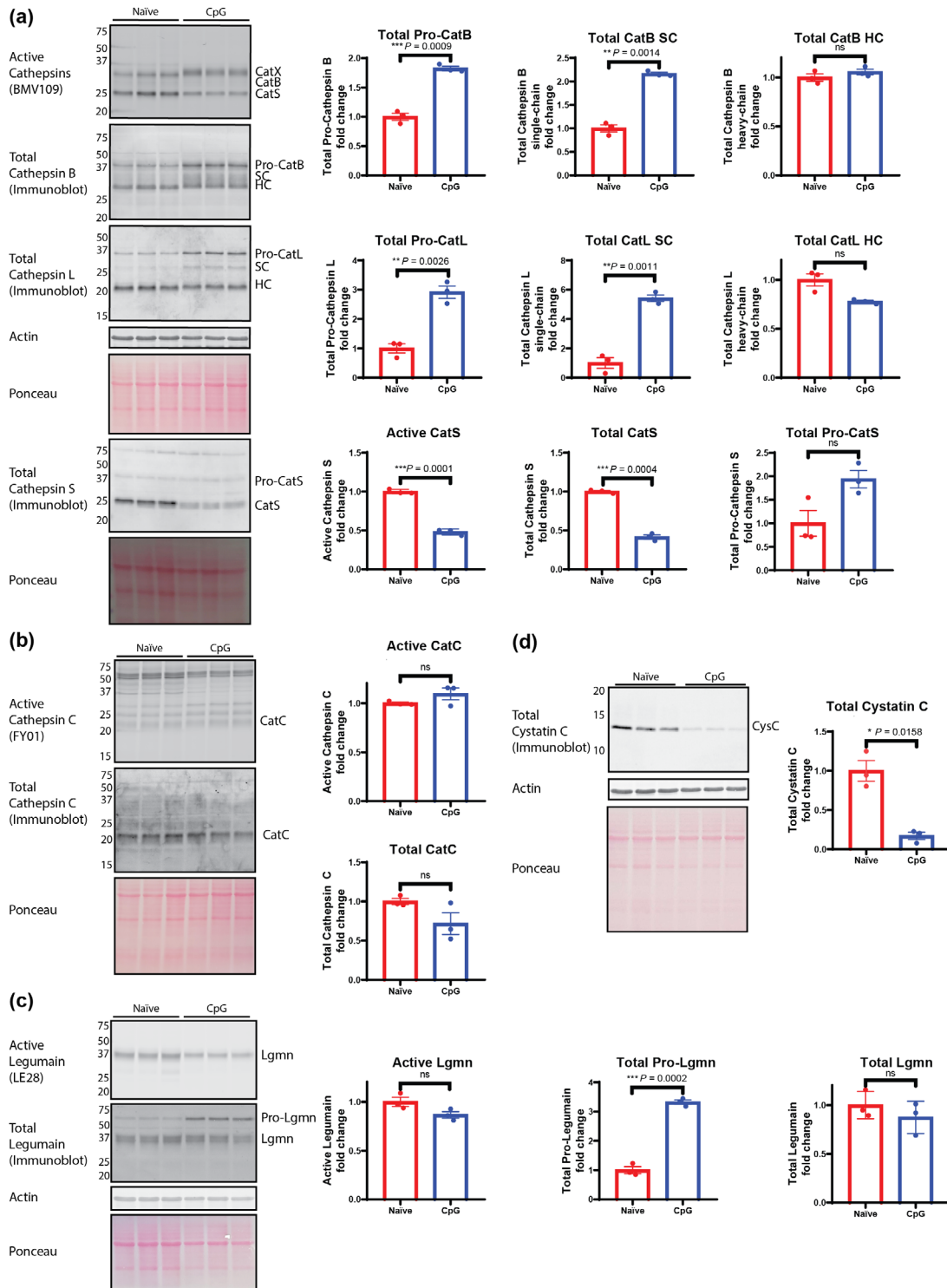


Figure 3. Cysteine proteases and cystatin C are differentially regulated during DC maturation. Mutu DCs were stimulated with CpG for 24 h, followed by BMV109 labeling and cathepsin B/L/S immunoblotting **(a)**, FY01 labeling and cathepsin C immunoblotting **(b)**, LE28 labeling and legumain immunoblotting **(c)** and cystatin C immunoblotting **(d)**. Actin and Ponceau stain were used to assess protein loading. Densitometry of the indicated bands were displayed as the average intensity for all naive and treated cells, relative to naive (fold change). Statistical analysis was performed using unpaired Student's *t*-tests. Three technical replicates of stimulated cells are shown, representative of > 3 separate experiments. Error bars represent SEM. ns $P > 0.05$, * $P \leq 0.05$, ** $P \leq 0.01$, *** $P \leq 0.001$.

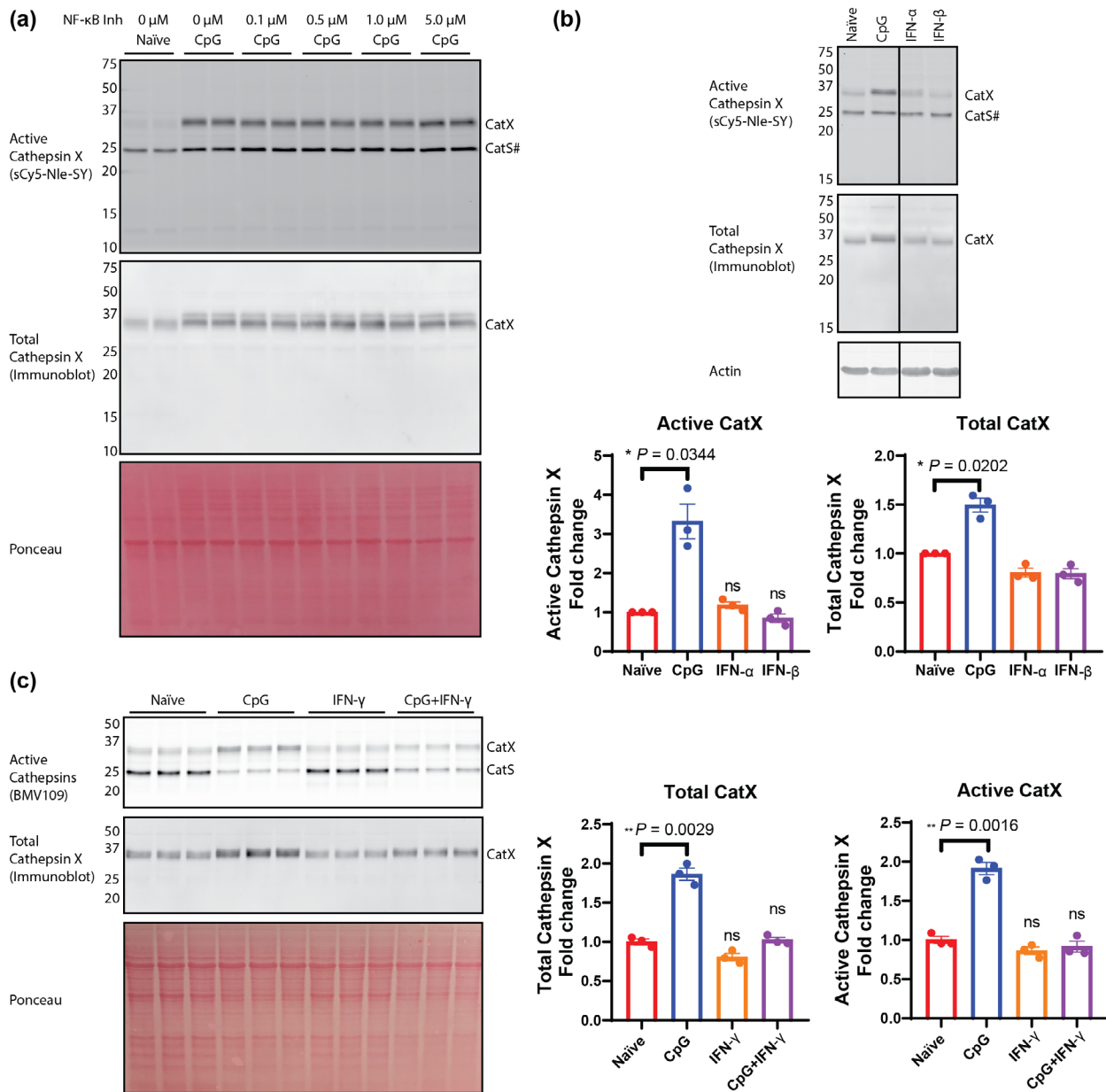


Figure 4. Effect of NF-κB inhibition and IFN treatment on cathepsin X upregulation. **(a)** Mutu DCs were pre-treated with the indicated concentration of NF-κB activation inhibitor for 4 h and CpG (0.5 μM) activation for 24 h, followed live labeling with sCy5-Nle-SY and analysis of in-gel fluorescence and cathepsin X immunoblotting. Ponceau stain was used to assess loading. **(b)** Mutu DCs were treated with CpG, IFN-α or IFN-β for 24 h, followed by sCy5-Nle-SY labeling and cathepsin X immunoblotting. Densitometry of active and total cathepsin X bands displayed as the average intensity for all naïve and treated cells relative to naïve cells (fold-change). Statistical analysis was performed using unpaired Student's *t*-tests. Three technical replicates of stimulated cells are shown, representative of > 3 separate experiments. **(c)** Mutu DCs were pre-treated with CpG, IFN-γ or a combination of CpG and IFN-γ for 24 h, followed by sCy5-Nle-SY labeling and cathepsin X immunoblotting. Ponceau stain was used to assess loading. Densitometry of active and total cathepsin X displayed as the average intensity for all naïve and treated cells relative to naïve cells (fold-change). Statistics were performed using unpaired Student's *t*-tests. Three technical replicates of stimulated cells are shown, representative of > 3 separate experiments. Error bars represent SEM. ns *P* > 0.05, **P* ≤ 0.05, ***P* ≤ 0.01. #This band may be a mixture of cathepsin S and another protease.

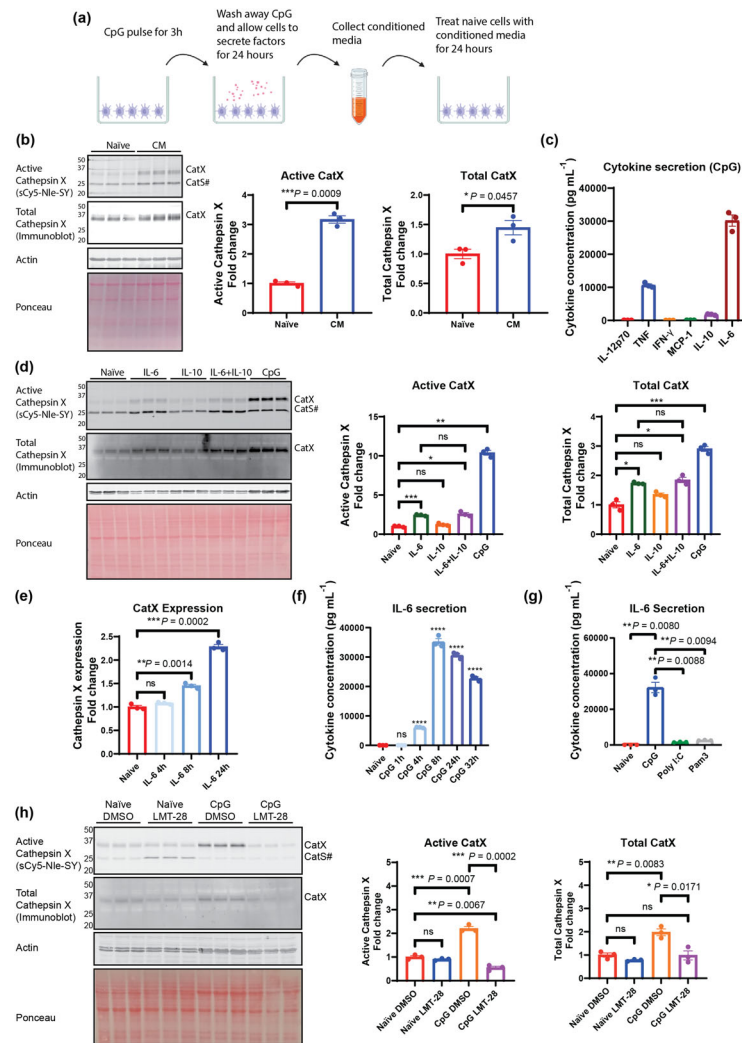


Figure 5. IL-6 secreted by DCs in response to TLR9 activation promotes cathepsin X upregulation. **(a, b)** Experimental set-up and subsequent analysis. Naïve Mutu DCs were treated with CpG for 3 h and washed. Conditioned media was collected for 24 h and applied to naïve cells for a further 24 h. After live labeling with sCy5-Nle-SY, protein was analyzed by in-gel fluorescence followed by cathepsin X immunoblotting. Actin and Ponceau stain were used to assess loading. Densitometry of active and total cathepsin X displayed as the average intensity for all naïve and treated cells relative to naïve cells (fold-change). Statistical analysis was performed using unpaired Student's *t*-tests. Three technical replicates of stimulated cells are shown, representative of > 3 separate experiments. **(c)** Mutu DCs were treated with CpG for 24 h, and the concentration of IL-12 p70, TNF α , IFN- γ , MCP-1, IL-10 and IL-6 in conditioned media was analyzed with the BD[®] Cytometric Bead Array. **(d)** Mutu DCs were treated with IL-6, IL-10, CpG or a combination of IL-6 and IL-10 for 24 h, followed by sCy5-Nle-SY labeling and cathepsin X immunoblotting. Ponceau stain was used to assess loading. Densitometry of active and total cathepsin X displayed as the average intensity for all naïve and treated cells relative to naïve cells (fold-change). Statistical analysis was performed using unpaired Student's *t*-tests. Three technical replicates of stimulated cells are shown, representative of > 3 separate experiments. **(e)** Quantitative PCR analysis of cathepsin X mRNA normalized to mouse GAPDH in naïve and IL-6-treated Mutu DCs, reported as fold-change compared with naïve. Statistical analysis was performed using unpaired Student's *t*-tests. Three technical replicates of stimulated cells are shown, representative of two separate experiments. **(f)** Time course of IL-6 secretion by Mutu DCs stimulated with CpG. Statistical analysis was performed using the Brown–Forsythe and Welch ANOVA tests. Three technical replicates of stimulated cells are shown. **(g)** Secretion of IL-6 by Mutu DCs stimulated with CpG, Poly I:C or PAM3 for 24 h. Statistical analysis was performed using Student's *t*-test. Three technical replicates of stimulated cells are shown, representative of two separate experiments. **(h)** Naïve or CpG-stimulated Mutu DCs were treated with LMT-28 or DMSO vehicle for 8 h prior to stimulation with CpG for 16 h and subsequent analysis of cathepsin X activity and expression by immunoblotting. Ponceau stain was used to assess loading. Densitometry of active and total cathepsin X displayed as the average intensity for all cells relative to naïve cells (fold-change). Statistical analysis was performed using unpaired Student's *t*-tests. Three technical replicates of stimulated cells are shown, representative of three separate experiments. Error bars represent SEM. ns $P > 0.05$, * $P \leq 0.05$, ** $P \leq 0.01$, *** $P \leq 0.001$, **** $P \leq 0.0001$. #This band may be a mixture of cathepsin S and another protease.

(Figure 5c). Secretion of IFN- γ , MCP-1 and IL-12 was negligible. IL-10 and IL-6, as well as IL-4 and IL-13, are known to promote STAT3/6-dependent expression of several cathepsins in macrophages.¹⁵ We tested whether these cytokines could similarly affect cathepsin X expression in DCs. Treatment with IL-6, but not IL-4 or IL-10, significantly increased active and total cathepsin X (2.4-fold, $P = 0.0002$ and 1.7-fold, $P = 0.0383$) (Figure 5d; Supplementary figure 6). By quantitative PCR, we observed that IL-6 provoked cathepsin X mRNA expression in a time-dependent manner, with significant increases detected after 8 h (1.5-fold, $P = 0.0014$) and 24 h (2.3-fold, $P = 0.0002$), but not as early as 4 h (Figure 5e). Secretion of IL-6 was increased at 4 h post-CpG administration and peaked at 8 h (Figure 5f), suggesting that IL-6 secretion precedes cathepsin X upregulation. As Poly I:C and PAM3 treatments did not elicit a robust increase in cathepsin X (Figure 1a–c), we compared the level of IL-6 secretion between CpG-, Poly I:C- and PAM3-treated DCs. Cells treated with CpG secreted significantly more IL-6 compared with Poly I:C or PAM3 (20.1-fold, $P = 0.0088$ and 12.3-fold, $P = 0.0094$, respectively) (Figure 5g). As such, IL-6 and cathepsin X levels correlate across these three agonists.

Finally, to investigate whether IL-6 was the factor responsible for provoking cathepsin X expression upon CpG-induced DC maturation, we treated naïve or CpG-activated Mutu DCs with a small-molecule inhibitor of IL-6 signaling, LMT-28, which binds to the IL-6 receptor β subunit, glycoprotein 130 (gp130), to suppress STAT3 phosphorylation.⁴⁰ Strikingly, LMT-28 treatment completely prevented the CpG-mediated upregulation of cathepsin X. In fact, co-treated DCs exhibited slightly less cathepsin X activity than naïve DCs (0.6-fold, $P = 0.0067$), as opposed to the 2.2-fold increase observed with CpG alone ($P = 0.0007$), suggesting IL-6 may impact basal cathepsin X expression. Collectively, these results demonstrate a critical role for IL-6 in regulating cathepsin X expression during TLR9-induced DC maturation.

DISCUSSION

We have demonstrated that cathepsin X is upregulated to different extents during the maturation of Mutu DCs in response to different TLR agonists. We observed that total and active cathepsin X levels were increased by some agonists, but this was not directly proportional to the DC maturation status indicated by cell surface CD86 levels. CpG, Pam3, FSL-1 and Poly I:C all stimulated Mutu DCs to a similar extent; however, upregulation of cathepsin X activity varied widely (11.2-, 4.7-, 7.0- and 2.6-fold, respectively). We hypothesize that the

discrepancy in cathepsin X expression may be due to differences in signaling nodes activated downstream of TLR agonists. TLR1/2 (Pam3), TLR 2/6 (FSL-1) and TLR 9 (CpG) all engage the MyD88 adaptor protein, while TLR 3 (Poly I:C) recruits TRIF.³⁹ MyD88 and TRIF-dependent signaling pathways ultimately activate two transcription factors: NF- κ B and IRFs. The MyD88-dependent signaling cascade is inclined to NF- κ B activation and, subsequently, the transcription of pro-inflammatory genes such as interleukins. The TRIF-dependent pathway, however, is skewed towards IRF activation and triggers the expression of type I interferons (e.g. IFN- β).⁴¹ We aimed to explore the signaling mechanisms underpinning the differential cathepsin X responses downstream of TLR agonism.

Upregulation of cathepsin X was observed well after CpG stimulation (24 h), while NF- κ B-dependent cytokine secretion was detected as early as 4 h post-CpG treatment. As a result, we speculated that upregulation of cathepsin X was not the direct result of NF- κ B-mediated transcription. In support of this, treatment of Mutu DCs with an NF- κ B inhibitor had no impact on cathepsin X upregulation in response to CpG, despite it being able to reduce cytokine production by 29–62%.

As inflammatory cytokines are known to increase the expression of multiple lysosomal proteases in macrophages through STAT3- and STAT6-dependent mechanisms,¹⁵ we hypothesized that cytokines secreted by DCs in response to CpG might be the drivers of cathepsin X expression. Indeed, factors produced by cells pulsed with CpG for only 3 h provoked an increase in cathepsin X expression. We found that IL-6, but not IL-4, IL-10, IFN- α or IFN- β , promoted the expression of both cathepsin X mRNA and protein. These results suggest that cathepsin X upregulation was not directly due to TLR agonism but rather a secondary effect provoked by secreted IL-6. In support of this, blockade of IL-6 receptor signaling was able to completely reverse CpG-dependent increase in cathepsin X. In fact, inhibition of this pathway reduced cathepsin X to below the levels of naïve cells, suggesting that even very low levels of IL-6 can provoke cathepsin X expression. This potency may explain why the observed 30% decrease in IL-6 after NF- κ B inhibition had no effect on cathepsin X. Compared with CpG-activated DCs, Poly I:C and PAM3 treatment led to significantly less IL-6 secretion, which mirrored cathepsin X levels. Collectively, these data demonstrate that IL-6 levels govern the extent of cathepsin X expression in response to these agonists.

In macrophages, co-treatment of IL-6 and IL-10 led to a synergistic increase in cathepsin X expression compared with either cytokine alone.¹⁵ In Mutu DCs, however, IL-10 secretion was very low, and treatment

with recombinant IL-10, alone or in combination with IL-6, had no effect on cathepsin X expression. As CpG treatment is known to provoke IL-6 secretion in macrophages,⁴² we predict that cathepsin X activity will be similarly induced in these cells, although this is an area for further investigation.

T_H2-associated cytokines such as IL-6 also provoke Irel α -dependent cathepsin secretion in macrophages. In Mutu DCs, we observed a CpG-mediated increase in cathepsin X secretion. Whether this is due to the overall increase in cathepsin X transcription or to activation of secretion pathways downstream of IL-6, via IRE1 α or otherwise, will require future investigation. Under normal cell culture conditions, extracellular cathepsin X is present mainly in its inactive zymogen form. Cathepsin X requires an acidic environment to be active and may not be capable of cleaving extracellular substrates in normal physiological conditions. In the context of an acidic cancer microenvironment, it is anticipated that extracellular cathepsin X may be activated to cleave substrates,⁴³ although evidence of this is currently limited. The pro-peptide sequence of cathepsin X contains an RGD motif that likely signals independent of its proteolytic functions. The RGD motif can bind to β 2 integrin receptors to promote cell proliferation and to α 5 integrin receptors to facilitate NLRP3-dependent inflammasome activation.^{21,44} Whether or not the RGD motif contributes to DC function is not currently known, although cleavage of the Mac-1 integrin receptor by cathepsin X has been implicated in DC adhesion and migration.¹⁹

In addition to cathepsin X, we investigated the active and total levels of other lysosomal proteases in CpG-mediated DC maturation. We used a pan-cysteine cathepsin probe BMV109 to measure the active level of cathepsin B, L, S and X. We observed inconsistencies in the labeling of cathepsin B and L between experiments; however, when they were observed, they were always labeled at much lower levels than cathepsin X and S. By immunoblotting, we found that the pro- and single-chain forms of cathepsin B and L were significantly elevated, while the mature double chain forms of cathepsin B and L were unchanged. Labeling of cathepsin S by BMV109 was reduced after CpG treatment, while sCy5-Nle-SY labeling was conversely increased. Further investigation by immunoblot revealed that the level of mature cathepsin S was decreased. We speculate that the 25 kDa band arising from sCy5-Nle-SY labeling consists of cathepsin S and additional protease(s) exhibiting the same size and MDV-590 reactivity. Alternatively, the two probes may traffic to different compartments within the cells, which could affect the labeling profiles. This inconsistency will need to be addressed in future with

chemical proteomics and microscopy-based approaches. We are confident that the 35 kDa band labeled by sCy5-Nle-SY is cathepsin X, due to the complete immunoprecipitation of this species with a cathepsin X antibody and the observation that this species is completely absent in cathepsin X-deficient Mutu DCs.²⁶

The function of cathepsin X within different DC subsets, and why it might be differentially regulated in response to different pathogen-associated molecular patterns, is still an open question. Only a few substrates for cathepsin X have been identified to date, and many of them have not been verified under physiological conditions. A more complete understanding of its function will require systematic identification of substrates that are cleaved by cathepsin X *in situ*, whether in the lysosome, cytosol or outside the cell. IL-6 is produced by many types of immune cells including T cells, monocytes, macrophages, as well as tumor cells. In addition to its cell intrinsic effects, it will also be important to examine the paracrine regulation of cathepsin X by IL-6 within DCs, and how its substrate profile changes in the context of infection and disease.

METHODS

Cell culture

Mutu DCs²⁴ were cultured in Iscove's Modified Dulbecco's Medium (IMDM; Gibco; Scoresby, Australia) supplemented with 10% (v/v) fetal bovine serum (FBS), 60 μ g mL⁻¹ penicillin, 100 μ g mL⁻¹ streptomycin and 100 μ M β -mercaptoethanol.^{24,45} For passaging, the cells were lifted from the flask using ethylenediaminetetraacetic acid-balanced salt solution (EDTA-BSS; 150 mM sodium chloride, 4 mM potassium chloride, 24 μ M disodium hydrogen orthophosphate, 12 μ M sodium dihydrogen orthophosphate, 15 mM HEPES and 5 mM EDTA (The Peter Doherty Institute for Infection and Immunity media preparation unit [MPU]; Melbourne, Australia) supplemented with 2% (v/v) FBS).

Mice

All experiments involving animals were conducted under the guidelines for using laboratory animals in research and protocols approved by the University of Melbourne Animal Ethics Committee. C57BL/6 mice were obtained from the Melbourne Bioresources Platform at Bio21 Molecular Science and Biotechnology Institute.

Dendritic cell stimulation

1×10^6 Mutu DCs were plated in 6-well plates overnight followed by the addition of stimuli for 24 h (or otherwise indicated): 0.5 μ M CpG (Bioneer; Kew East, Australia), 1 μ g mL⁻¹ LPS (14 011, Cell Signaling; Notting Hill,

Australia), 100 $\mu\text{g mL}^{-1}$ Poly I:C (INV-tlr-pic, Invivogen; San Diego, USA), 500 ng mL^{-1} Pam3CSK4 (tlrl-pms, Invivogen), 500 ng mL^{-1} FSL-1 (tlrl-fsl, Invivogen), 2 $\mu\text{g mL}^{-1}$ R848 (tlrl-r848, Invivogen), 20 ng mL^{-1} IL-4 (214-14-20, Peprotech; Norwest, Australia), 20 ng mL^{-1} IL-6 (406-ML-005, R&D Systems), 20 ng mL^{-1} IL-10 (RMIL105 Invitrogen; Scoresby, Australia), 5000 U mL^{-1} IFN- α (121001, Invitrogen), 50 ng mL^{-1} IFN- β (8234-MB/CF, R&D Systems; Minneapolis, USA) and 50 ng mL^{-1} IFN- γ (315-05-100, Peprotech).

Inhibition of NF- κ B or IL-6R activation

NF- κ B Activation Inhibitor, 6-amino-4-(4-phenoxyphenylethylamino) quinazoline (481406, Calbiochem[®]; Bayswater, Australia) was reconstituted in DMSO with an initial concentration of 50 mM. NF- κ B Activation Inhibitor was diluted from 1000 \times DMSO stock and administered directly into cell culture (0.1% final DMSO) 4 h before the addition of CpG. The final concentration used is indicated in the relevant section. IL-6R inhibitor, LMT-28 (HY-102084, MedChemExpress; Monmouth Junction, USA) was reconstituted in DMSO. LMT-28 (100 μM) was diluted from 1000 \times DMSO stock and administered directly into cell culture (0.1% final DMSO) 8 h before the addition of CpG.

Detection of protease activity using activity-based probes and in-gel fluorescence

The following activity-based probes were dissolved in DMSO and added to the cell media 4 h before harvesting (final concentration 1 μM , 0.1% DMSO): sCy5-Nle-SY (cathepsin X and S selective),²⁵ BMV109 (cathepsin X, B, S, L),^{28,29} FY01 (cathepsin C)³⁰ or LE28 (legumain).³¹ Where indicated, the cells were pre-treated with the cathepsin S inhibitor MDV-590²⁷ for 24 h before probe addition. Cells were collected, washed with PBS to remove excess probe and serum, and lysed with PBS containing 0.1% Triton X-100. The cell lysates were cleared of debris by centrifugation at max speed for 7 min, and the supernatants were transferred to a new tube. A BCA assay (Thermo Fisher; Scoresby, Australia) was used to determine the total protein concentration using FLUOstar[®] (BMG LABTECH; Mornington, Australia). Sample buffer (1 \times : 10% glycerol, 50 mM Tris-Cl, pH 6.8, 2% SDS, 0.01% bromophenol blue, 1.25% beta-mercaptoethanol) was added to each sample from a 5 \times stock, followed by heating for 5 min at 95°C. Equal protein amounts (in general 80 μg) were resolved on 15% SDS-PAGE gels poured in-house. The gels were scanned for Cy5 fluorescence using a Typhoon 5 (GE Healthcare; Parramatta, Australia).

Analysis of conditioned media

The cells were washed with and plated in serum-free media (1 $\times 10^6$ cells/well in 6-well plates) and media was conditioned for 24 h. Conditioned media (CM) was collected, centrifuged at 300 g for 5 min to remove cell debris, and concentrated using Amicon[®] Ultra 0.5 mL 3 kDa centrifugal

filters (Millipore; Bayswater, Australia) according to the manufacturer's instructions. A BCA assay was used to determine the total protein concentration using FLUOstar[®] (BMG LABTECH). A total of ~ 80 μg protein was resolved by SDS-PAGE as above.

Immunoblotting

Proteins were transferred from gels to nitrocellulose membranes using a Trans-Blot Turbo Transfer System (BioRad; South Granville, Australia) in transfer buffer (1 \times Trans-Blot[®] Turbo[™] Transfer Buffer [BioRad] containing 20% ethanol). Membranes were incubated in primary antibodies overnight at 4°C: cathepsin X (AF1033, R&D Systems), cathepsin S (AF1183, R&D Systems), cathepsin B (AF965, R&D Systems), cathepsin L (AF1515, R&D Systems), cathepsin C (AF1034, R&D Systems), legumain (AF2058, R&D Systems) and cystatin C (AF1238, R&D Systems), all diluted at 1:1000. β -Actin (MA5-15739, Life Technologies; Mulgrave, Australia) was diluted at 1:10 000. The membranes were washed with PBS containing 0.05% Tween-20 (PBST) three times followed by incubation with secondary antibody on an orbital shaker for 1 h at room temperature: donkey anti-goat HRP (A15999, Invitrogen) and donkey anti-rabbit IRDye 800CW (92632213, Licor; Lincoln, USA), all diluted at 1:10 000. Membranes were then washed three times using PBST and once with PBS. IR800 immunoblots were scanned using Typhoon 5 (GE Healthcare). HRP labeling was visualized on a ChemiDoc[®] MP imager (BioRad; South Granville, Australia) using Pierce ECL Western blotting reagents (Thermo Fisher).

Immunofluorescence

Chamber slides (80826, Ibidi; Gräfelfing, Germany) were washed twice with 250 μL PBS and once with 250 μL IMDM. Cells (25 000) were added to each chamber in 250 μL media and incubated overnight. The attached cells were washed twice with 150 μL PBS and fixed with 150 μL 4% paraformaldehyde in PBS at room temperature for 10 min. The cells were then permeabilized with 150 μL 0.1% Triton X-100 at room temperature for 3 min, washed with PBS, and blocked with 10% normal horse serum (NHS) in PBS at room temperature for 30 min. Primary antibody diluted in 150 μL blocking buffer (1:200) was added to each chamber and incubated at 4°C overnight. Cells were washed twice with 150 μL 0.1% Triton X-100 in PBS followed by the addition of secondary antibody (donkey anti-goat 568, A-11057, Thermo Fisher; diluted 1:1000 in blocking buffer) at room temperature for 1 h. The cells were washed twice with 150 μL 0.1 Triton X-100 in PBS and nuclei were stained with DAPI in PBS (1 $\mu\text{g mL}^{-1}$) at room temperature for 5 min. After washing with PBS 3 times, the cells were stored in mounting buffer (90% glycerol in PBS) and imaged using the Leica SP8 Confocal Microscope (Leica; Macquarie Park, Australia) with a 63 \times /1.40 oil objective.

RNA isolation, cDNA synthesis and quantitative real-time PCR

Cathepsin X mRNA expression was analyzed as described previously.²⁶ Briefly, total RNA was extracted using Trizol, and genomic DNA was removed using DNase (Thermo Scientific, EN0521). cDNA was synthesized using a kit (Promega, A5001; Alexandria, Australia). All primers were designed using Primer 3 (National Center for Biotechnology Information) and verified by Primer Blast (NIH). GAPDH (F, 5'-GGTGCTGAGTATGTCGTGGA-3'; R, 5'-CGGAGATGATGACCCTTTTG-3') was used as a housekeeping gene control; cathepsin X (F, 5'-GGATTGTCCGAAATTCATGG-3'; R, 5'-ACTCTCGATGGC AAGGTTGT-3') was amplified with the QuantStudio™ 6 system (Thermo Fisher) using the following PCR conditions: 95°C for 3 min; 45 cycles of 95°C for 15 s and 60°C for 20 s. All mRNA levels were presented relative to GAPDH.

Cytokine quantification

1×10^6 Mutu DCs were plated in a 6-well plate and cultured overnight for attaching. The cells were then treated with CpG for the indicated time. Conditioned media was then collected and briefly centrifuged to remove cell debris. The conditioned media was subsequently analyzed with BD™ Cytometric Bead Array (CBA). The Mouse Inflammation Kit (BD, 552364; Mulgrave, Australia) was used according to the manufacturer's instructions.

Immunoprecipitation

Cells were live labeled with 1 μ M sCy5-Nle-SY and lysates were prepared. Total protein (40 μ g) was aliquoted into input and pulldown samples. The pulldown samples were diluted in IP buffer (PBS [pH 7.4], 0.5% NP-40 (v/v), 1 mM EDTA). Goat anti-cathepsin X (1:100, AF1033, R&D Systems) or goat anti-cathepsin S (1:50, AF1183, R&D Systems) was added along with a slurry of pre-washed Protein A/G agarose beads (Santa Cruz; Dallas, USA). Samples were rotated overnight at 4°C. After washing four times with IP buffer and once with 0.9% NaCl (w/v), the beads were resuspended in 2 \times sample buffer and boiled. The pulldown supernatants, along with the input samples, were analyzed by in-gel fluorescence as above.

Harvesting primary splenic dendritic cells

Splenic DCs were harvested as described by Vremec.⁴⁶ Briefly, spleens from naïve C57BL/6 mice were digested with 1 mg mL⁻¹ DNase I (Boehringer Mannheim; North Ryde, Australia) and 7 mg mL⁻¹ Collagenase Type III (Worthington, Lakewood, USA) for 20 min at room temperature in KDS-RPMI-FBS (potassium dodecyl sulphate Roswell Park Memorial Institute; RPMI 1640 containing 33.6 mM HEPES, 1 mM sodium pyruvate, 24 mM NaHCO₃, 2% (v/v) FBS). Cell clumps were separated with 100 mM EDTA treatment for 5 min at room temperature. DCs were purified from blood

cells by density gradient centrifugation in 1.977 g cm⁻³ Nycodenz (Nycomed Pharma; Macquarie Park, Australia). The DC populations were selected using a negative selection method by anti-rat-IgG-coupled magnetic beads (BioRad) and surface molecule antibodies (anti-mouse CD3, 1:100; anti-mouse CD90, 1:50; anti-mouse erythroid lineage, 1:10; anti-mouse Ly6G & Ly6C, 1:50; anti-mouse CD45R/B220, 1:100, WEHI antibody factory facility). To assess purity, the cells were stained with CD11c antibody (PE561, 1:400, BioLegend; Wangara, Australia) in the dark on ice for 20 min. Cells were washed with EDTA-BSS twice to remove excess antibodies, followed by propidium iodide (PI) staining (0.5 μ g mL⁻¹, Calbiochem) to distinguish live/dead cells. Sample acquisition was carried out on LSR Fortessa (BD Bioscience). Cell populations were identified based on their forward and side scatter, with cell viability determined by negative staining with PI. The DC purity assessed by CD11c staining was above 90%. Primary cells were cultured at 37°C and 10% CO₂ in RPMI 1640 supplied with 33.6 mM HEPES, 24 mM sodium bicarbonate (NaHCO₃), 60 μ g mL⁻¹ penicillin, 100 μ g mL⁻¹ streptomycin and 100 μ M β -mercaptoethanol. Primary splenic DCs (1×10^6 cells mL⁻¹ density) were stimulated with CpG (5 μ M) for 24 h.

Statistical analysis

Statistical analyses were performed using GraphPad Prism 8. Unpaired *t*-tests were performed to analyze differences between two groups. Ordinary one-way ANOVA followed by Dunnett's multiple comparisons test was used to compare more than two groups where indicated. Mean data points are expressed as mean \pm SEM. *P* < 0.05 was considered significant.

ACKNOWLEDGMENTS

We thank the Biological Optical Microscopy Platform and the Melbourne Bioresources and Cytometry Platforms at the Bio21 Institute. This work was supported by a Grimwade Research Fellowship funded by the Russell and Mab Grimwade Miegunyah Fund, an Australian Research Council DECRA fellowship (DE180100418) and a National Health and Medical Research Council Ideas Grant (GNT2011119) awarded to LEE-M. Open access publishing is facilitated by The University of Melbourne, as part of the Wiley – University of Melbourne agreement via the Council of Australian University Librarians.

AUTHOR CONTRIBUTIONS

Bangyan Xu: Data curation; formal analysis; investigation; methodology; validation; visualization; writing – original draft. **Bethany M Anderson:** Methodology; project administration; writing – review and editing. **Justine D Mintern:** Methodology; resources; supervision. **Laura E Edgington-Mitchell:** Conceptualization; project administration; resources; supervision; writing – review and editing.

CONFLICT OF INTEREST

The authors declare no competing interests.

DATA AVAILABILITY STATEMENT

All data reported in this manuscript are available upon request by contacting the corresponding author.

REFERENCES

- Pečar Fonović U, Kos J. Cathepsin X cleaves profilin 1 C-terminal Tyr139 and influences clathrin-mediated endocytosis. *PLoS One* 2015; **10**: e0137217.
- Honey K, Rudensky AY. Lysosomal cysteine proteases regulate antigen presentation. *Nat Rev Immunol* 2003; **3**: 472–482.
- Rodriguez GM, Diment S. Role of cathepsin D in antigen presentation of ovalbumin. *J Immunol* 1992; **149**: 2894–2898.
- Bennett K, Levine T, Ellis JS, *et al.* Antigen processing for presentation by class II major histocompatibility complex requires cleavage by cathepsin E. *Eur J Immunol* 1992; **22**: 1519–1524.
- Honey K, Nakagawa T, Peters C, Rudensky A. Cathepsin L regulates CD4⁺ T cell selection independently of its effect on invariant chain: a role in the generation of positively selecting peptide ligands. *J Exp Med* 2002; **195**: 1349–1358.
- Pluger EB, Boes M, Alfonso C, *et al.* Specific role for cathepsin S in the generation of antigenic peptides *in vivo*. *Eur J Immunol* 2002; **32**: 467–476.
- Antoniou AN, Blackwood S-L, Mazzeo D, Watts C. Control of antigen presentation by a single protease cleavage site. *Immunity* 2000; **12**: 391–398.
- Riese RJ, Wolf PR, Brömme D, *et al.* Essential role for cathepsin S in MHC class II-associated invariant chain processing and peptide loading. *Immunity* 1996; **4**: 357–366.
- Garcia-Cattaneo A, Gobert F-X, Müller M, *et al.* Cleavage of Toll-like receptor 3 by cathepsins B and H is essential for signaling. *Proc Natl Acad Sci USA* 2012; **109**: 9053–9058.
- Ewald SE, Engel A, Lee J, Wang M, Bogyo M, Barton GM. Nucleic acid recognition by Toll-like receptors is coupled to stepwise processing by cathepsins and asparagine endopeptidase. *J Exp Med* 2011; **208**: 643–651.
- Sepulveda FE, Maschalidi S, Colisson R, *et al.* Critical role for asparagine endopeptidase in endocytic Toll-like receptor signaling in dendritic cells. *Immunity* 2009; **31**: 737–748.
- Ha S-D, Martins A, Khazaie K, Han J, Chan BMC, Kim SO. Cathepsin B is involved in the trafficking of TNF- α -containing vesicles to the plasma membrane in macrophages. *J Immunol* 2008; **181**: 690–697.
- Talukdar R, Sareen A, Zhu H, *et al.* Release of cathepsin B in cytosol causes cell death in acute pancreatitis. *Gastroenterology* 2016; **151**: 747–758.
- Burgener SS, Leborgne NGF, Snipas SJ, Salvesen GS, Bird PI, Benarafa C. Cathepsin G inhibition by Serpinb1 and Serpinb6 prevents programmed necrosis in neutrophils and monocytes and reduces GSDMD-driven inflammation. *Cell Rep* 2019; **27**: 3646–3656.
- Yan D, Wang H-W, Bowman RL, Joyce JA. STAT3 and STAT6 signaling pathways synergize to promote cathepsin secretion from macrophages via IRE1 α activation. *Cell Rep* 2016; **16**: 2914–2927.
- Gocheva V, Wang HW, Gadea BB, *et al.* IL-4 induces cathepsin protease activity in tumor-associated macrophages to promote cancer growth and invasion. *Genes Dev* 2010; **24**: 241–255.
- Mohamed MM, Cavallo-Medved D, Rudy D, Anbalagan A, Moin K, Sloane BF. Interleukin-6 increases expression and secretion of cathepsin B by breast tumor-associated monocytes. *Cell Physiol Biochem* 2010; **25**: 315–324.
- Nägler DK, Zhang R, Tam W, Sulea T, Purisima EO, Ménard R. Human cathepsin X: a cysteine protease with unique carboxypeptidase activity. *Biochemistry* 1999; **38**: 12648–12654.
- Obermajer N, Svajger U, Bogyo M, Jeras M, Kos J. Maturation of dendritic cells depends on proteolytic cleavage by cathepsin X. *J Leukoc Biol* 2008; **84**: 1306–1315.
- Allan ERO, Campden RI, Ewanchuk BW, *et al.* A role for cathepsin Z in neuroinflammation provides mechanistic support for an epigenetic risk factor in multiple sclerosis. *J Neuroinflammation* 2017; **14**: 103.
- Campden RI, Warren AL, Greene CJ, *et al.* Extracellular cathepsin Z signals through the $\alpha(5)$ integrin and augments NLRP3 inflammasome activation. *J Biol Chem* 2022; **298**: 101459.
- Pišlar A, Nedeljković BB, Perić M, Jakoš T, Zidar N, Kos J. Cysteine peptidase cathepsin X as a therapeutic target for simultaneous TLR3/4-mediated microglia activation. *Mol Neurobiol* 2022; **59**: 2258–2276.
- Liu H, Wilson KR, Firth AM, *et al.* Ubiquitin-like protein 3 (UBL3) is required for MARCH ubiquitination of major histocompatibility complex class II and CD86. *Nat Commun* 2022; **13**: 1934.
- Fuertes Marraco SA, Grosjean F, Duval A, *et al.* Novel murine dendritic cell lines: a powerful auxiliary tool for dendritic cell research. *Front Immunol* 2012; **3**: 331.
- Mountford SJ, Anderson BM, Xu B, *et al.* Application of a sulfoxonium ylide electrophile to generate cathepsin X-selective activity-based probes. *ACS Chem Biol* 2020; **15**: 718–727.
- Xu B, Anderson BM, Mountford SJ, Thompson PE, Mintern JD, Edgington-Mitchell LE. Cathepsin X deficiency alters the processing and localisation of cathepsin L and impairs cleavage of a nuclear cathepsin L substrate. *Biol Chem* 2024; **405**: 351–365.
- Hewitt E, Pitcher T, Rizoška B, *et al.* Selective cathepsin S inhibition with MIV-247 attenuates mechanical allodynia and enhances the antiallodynic effects of gabapentin and pregabalin in a mouse model of neuropathic pain. *J Pharmacol Exp Ther* 2016; **358**: 387–396.

28. Verdoes M, Oresic Bender K, Segal E, *et al.* Improved quenched fluorescent probe for imaging of cysteine cathepsin activity. *J Am Chem Soc* 2013; **135**: 14726–14730.
29. Edgington-Mitchell LE, Bogyo M, Verdoes M. Live cell imaging and profiling of cysteine cathepsin activity using a quenched activity-based probe. *Methods Mol Biol* 2017; **1491**: 145–159.
30. Yuan F, Verhelst SH, Blum G, Coussens LM, Bogyo M. A selective activity-based probe for the papain family cysteine protease dipeptidyl peptidase I/cathepsin C. *J Am Chem Soc* 2006; **128**: 5616–5617.
31. Edgington LE, Verdoes M, Ortega A, *et al.* Functional imaging of legumain in cancer using a new quenched activity-based probe. *J Am Chem Soc* 2013; **135**: 174–182.
32. Xu Y, Schnorrer P, Proietto A, *et al.* IL-10 controls cystatin C synthesis and blood concentration in response to inflammation through regulation of IFN regulatory factor 8 expression. *J Immunol* 2011; **186**: 3666–3673.
33. Tsujimura H, Tamura T, Kong HJ, *et al.* Toll-like receptor 9 signaling activates NF- κ B through IFN regulatory factor-8/IFN consensus sequence binding protein in dendritic cells. *J Immunol* 2004; **172**: 6820–6827.
34. Akkari L, Gocheva V, Quick ML, *et al.* Combined deletion of cathepsin protease family members reveals compensatory mechanisms in cancer. *Genes Dev* 2016; **30**: 220–232.
35. Tobe M, Isobe Y, Tomizawa H, *et al.* Discovery of quinazolines as a novel structural class of potent inhibitors of NF- κ B activation. *Bioorg Med Chem* 2003; **11**: 383–391.
36. Chen KY, Wang LC. Stimulation of IL-1 β and IL-6 through NF- κ B and sonic hedgehog-dependent pathways in mouse astrocytes by excretory/secretory products of fifth-stage larval *Angiostrongylus cantonensis*. *Parasit Vectors* 2017; **10**: 445.
37. Ernst O, Vayttaden SJ, Fraser IDC. Measurement of NF- κ B activation in TLR-activated macrophages. *Methods Mol Biol* 2018; **1714**: 67–78.
38. Son M, Frank T, Holst-Hansen T, *et al.* Spatiotemporal NF- κ B dynamics encodes the position, amplitude, and duration of local immune inputs. *Sci Adv* 2022; **8**: eabn6240.
39. Rakoff-Nahoum S, Medzhitov R. Toll-like receptors and cancer. *Nat Rev Cancer* 2008; **9**: 57.
40. Hong SS, Choi JH, Lee SY, *et al.* A novel small-molecule inhibitor targeting the IL-6 receptor β subunit, glycoprotein 130. *J Immunol* 2015; **195**: 237–245.
41. Yamamoto M, Sato S, Hemmi H, *et al.* Role of adaptor TRIF in the MyD88-independent Toll-like receptor signaling pathway. *Science* 2003; **301**: 640–643.
42. Liu M, O'Connor RS, Trefely S, Graham K, Snyder NW, Beatty GL. Metabolic rewiring of macrophages by CpG potentiates clearance of cancer cells and overcomes tumor-expressed CD47-mediated 'don't-eat-me' signal. *Nat Immunol* 2019; **20**: 265–275.
43. Estrella V, Chen T, Lloyd M, *et al.* Acidity generated by the tumor microenvironment drives local invasion. *Cancer Res* 2013; **73**: 1524–1535.
44. Akkari L, Gocheva V, Kester JC, *et al.* Distinct functions of macrophage-derived and cancer cell-derived cathepsin Z combine to promote tumor malignancy via interactions with the extracellular matrix. *Genes Dev* 2014; **28**: 2134–2150.
45. Wilson KR, Liu H, Healey G, *et al.* MARCH1-mediated ubiquitination of MHC II impacts the MHC I antigen presentation pathway. *PLoS One* 2018; **13**: e0200540.
46. Vremec D. The isolation of mouse dendritic cells from lymphoid tissues and the identification of dendritic cell subtypes by multiparameter flow cytometry. *Methods Mol Biol* 2010; **595**: 205–229.

SUPPORTING INFORMATION

Additional supporting information may be found online in the Supporting Information section at the end of the article.

© 2024 The Author(s). Immunology & Cell Biology published by John Wiley & Sons Australia, Ltd on behalf of the Australian and New Zealand Society for Immunology, Inc.

This is an open access article under the terms of the [Creative Commons Attribution](https://creativecommons.org/licenses/by/4.0/) License, which permits use, distribution and reproduction in any medium, provided the original work is properly cited.